

# Supplementary information

## *Design and synthesis of organic-inorganic hybrid capsules for biotechnological applications*

• Jiafu Shi<sup>a, b, §</sup>, Yanjun Jiang<sup>c, §</sup>, Xiaoli Wang<sup>a</sup>, Hong Wu<sup>a, d</sup>, Dong Yang<sup>a</sup>, Fusheng Pan<sup>a, d</sup>, Yanlei Su<sup>a, d</sup>, Zhongyi Jiang<sup>a, d, \*</sup>

• <sup>a</sup> Key Laboratory for Green Chemical Technology of Ministry of Education, School of Chemical Engineering and Technology, Tianjin University, Tianjin 300072, China.

• <sup>b</sup> School of Environmental Science and Engineering, Tianjin University, Tianjin 300072, China

• <sup>c</sup> School of Chemical Engineering and Technology, HeBei University of Technology, Tianjin 300130, China

• <sup>d</sup> Collaborative Innovation Center of Chemical Science and Engineering (Tianjin), Tianjin, 300072, China

• <sup>§</sup> Jiafu Shi and Yanjun Jiang contributed equally.

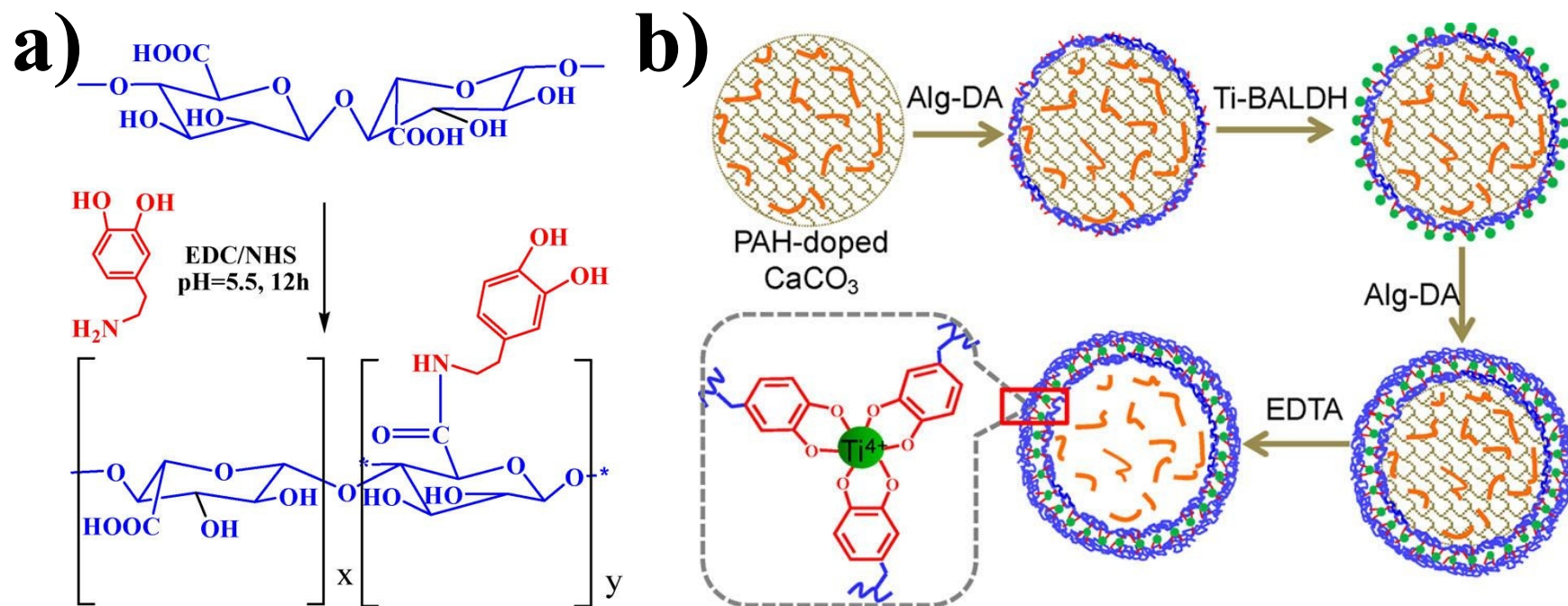


**Fig. S1** a) Schematic of representation of the synthesis process of dopamine modified alginate (Alg-DA) and b) the fabrication process of hybrid microcapsules. Reprinted with permission from ref. 19. Copyright 2012 American Chemistry Society.

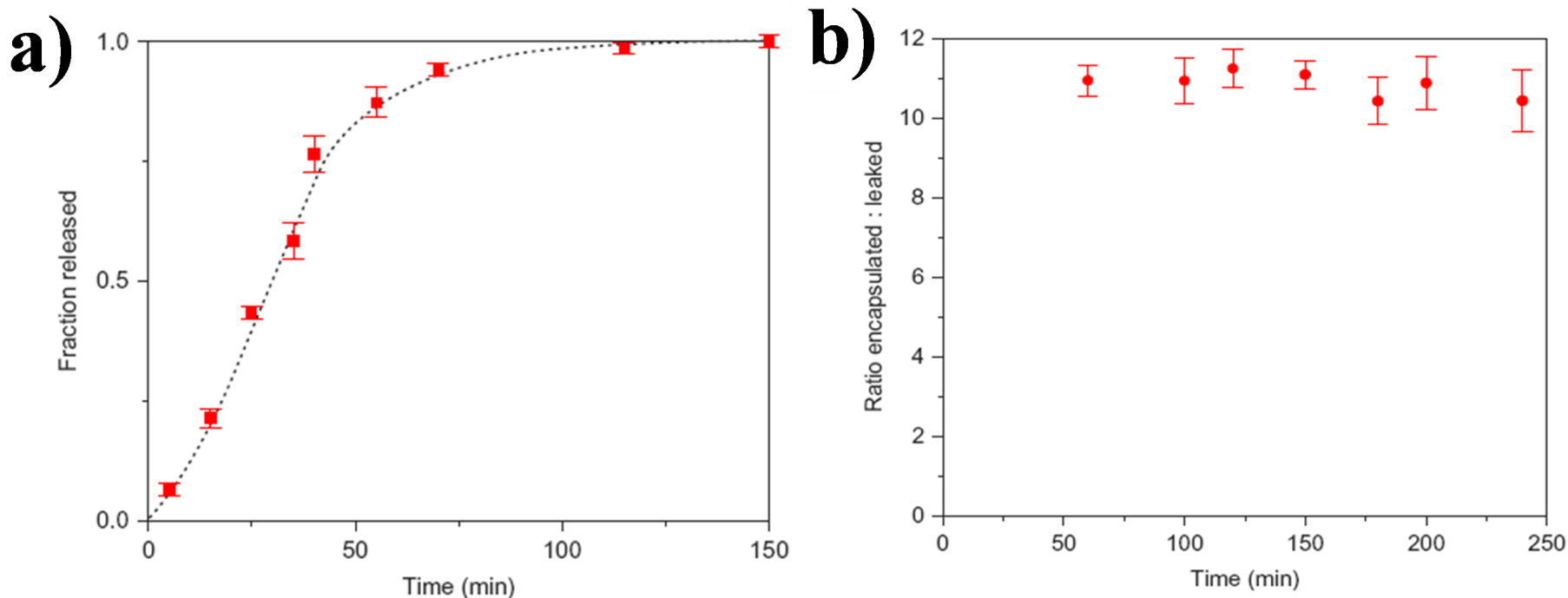


**Fig. S2** Selective permeability of [Cu<sub>3</sub>(BTC)<sub>2</sub>] MOF capsules. a) Release of the small molecule ethylene glycol through the capsule wall. Experimental data (red squares) are well described by a Fickian diffusion model (black squares) for a diffusivity of  $5 \times 10^{-11} \text{ cm}^2 \text{ s}^{-1}$  in the microporous capsule wall. b) Encapsulation of the large dye molecule Rose Bengal. The experimental ratio of dye molecules inside and outside the capsules (red circles) remains constant over time, confirming effective encapsulation. In both graphs, error bars indicate standard deviation. Reprinted with permission from ref. 20. Copyright 2011 Nature Publishing Group.

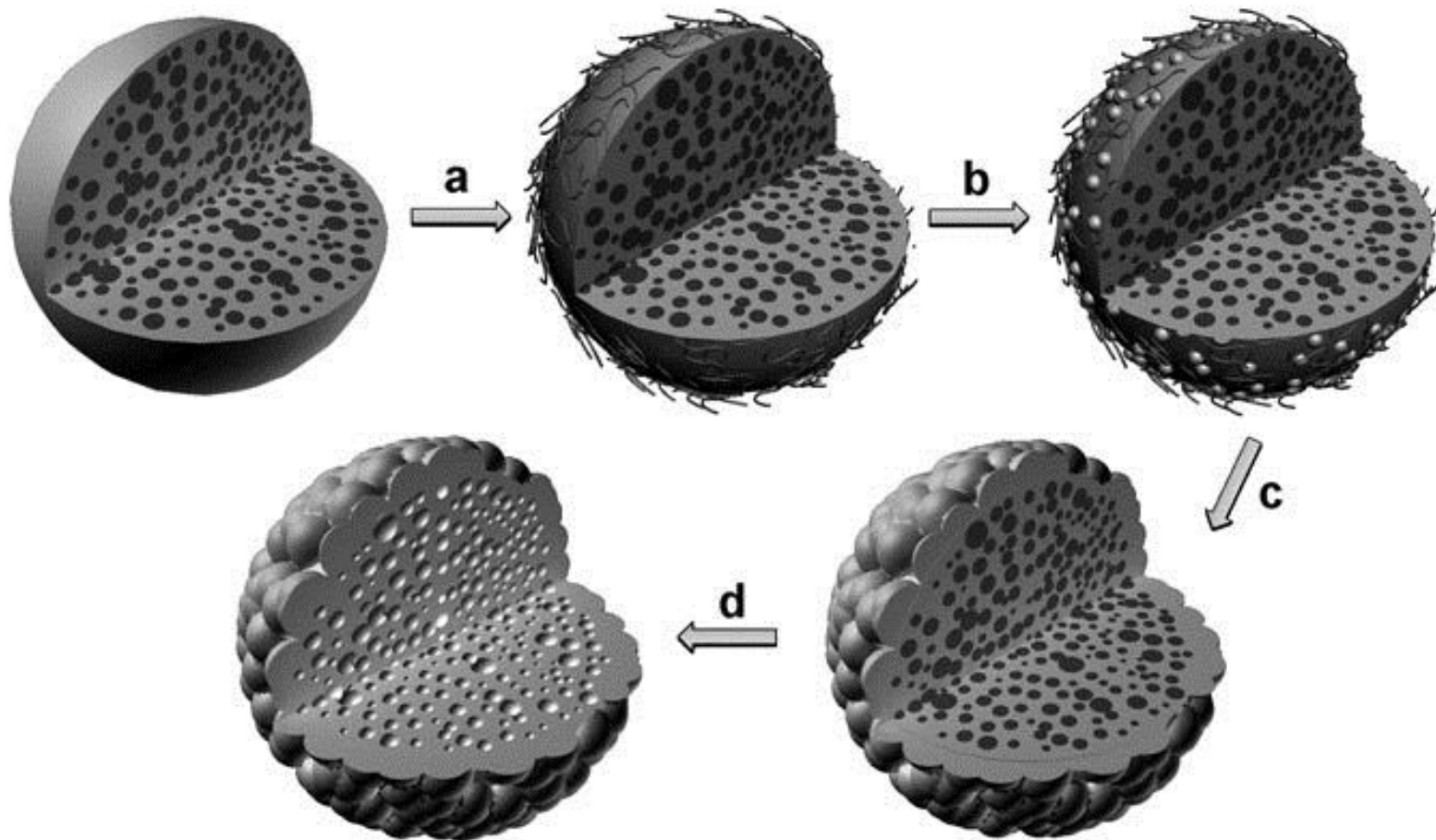


**Fig. S3** Fabrication process of gold-nanoshelled microcapsules: a) electrostatic adsorption of PAH onto microcapsules generated by the W/O/W double-emulsion method; b) deposition of gold nanoparticles onto PAH-coated microcapsules; c) formation of gold nanoshells by the surface-seeding method; d) lyophilization to sublimate the encapsulated water in the inner aqueous phase of the microcapsules to produce small hollow spaces. Reprinted with permission from ref. 26. Copyright 2011 Wiley-VCH.

**Table S1** List of the various polyamines, multivalent anions, shell materials and cargo that can be formulated into PSA-capsules. Reproduced from ref. 28.

Copyright 2011 Royal Society of Chemistry.

---

Polyamine	poly-L-lysine, poly-L-arginine, poly-L-histidine, poly-L-ornithine, chitosan, polyallylamine hydrochloride, branched-polyethyleneimine
Multivalent anion	phosphate, sulfate, succinnate, isocitrate, citrate, tri-carballylate, trimesate, ethylenediamine tetraaceticacid (EDTA), $\text{Na}_5(\text{Asp})_4$ , tripolyphosphate, Gd–DOTP
Shell material	$\text{SiO}_2$ , $\text{SnO}_2$ , ZnO, CdSe, $\text{Fe}_3\text{O}_4$ , polyacrylic acid, poly-styrene sulfonate, poly-L-glutamic acid, heparin, polygalacturonic acid, anti-EGFR, human serum albumin, bovine serum albumin, lactalbumin

---

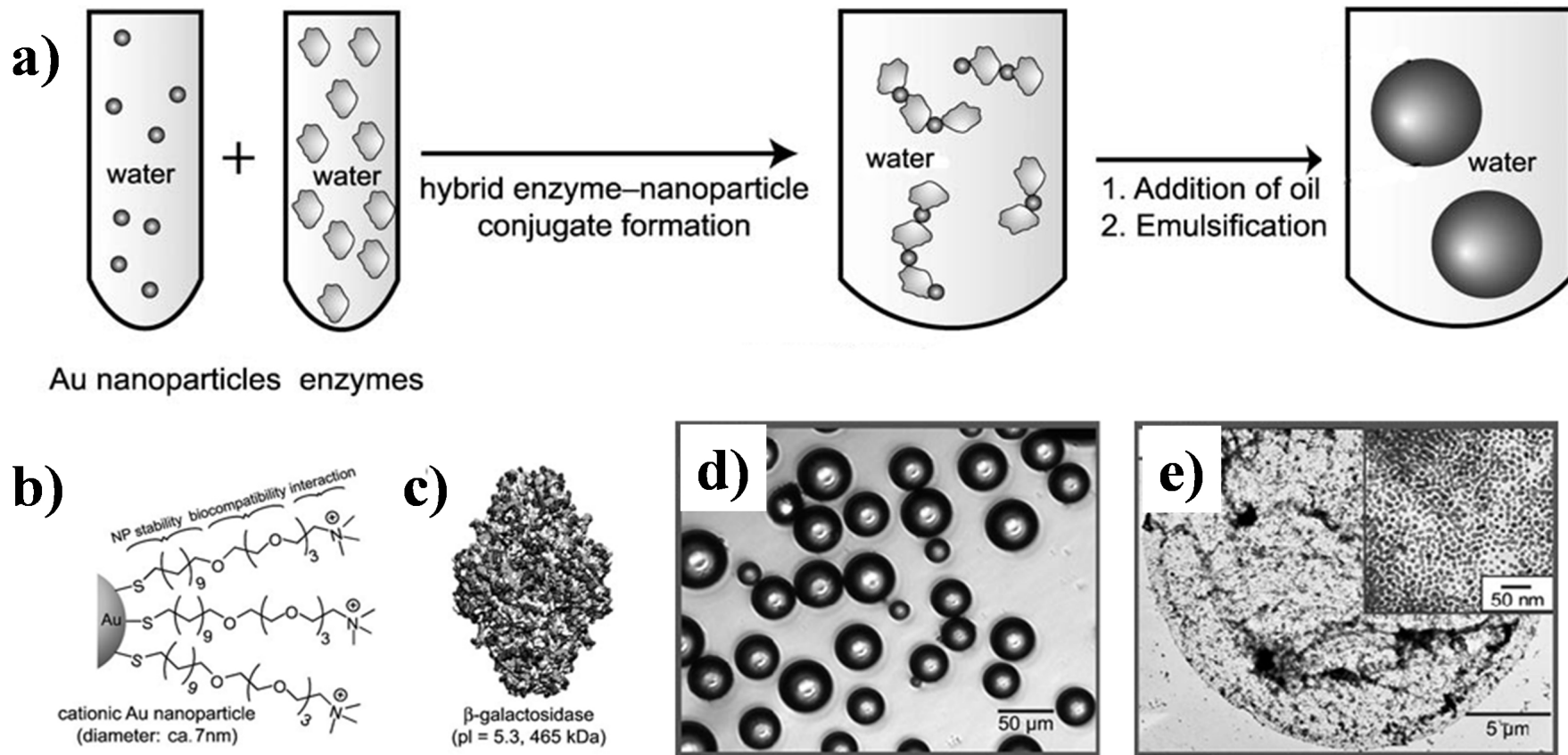


**Fig. S4** a) Formation of enzymatic capsules through electrostatic assembly of enzymes and nanoparticles in water followed by assembly of the resulting enzyme-nanoparticle conjugates at oil-water interfaces; b) structure of  $\beta$ -gal; c) chemical structure of cationic gold nanoparticles; d) optical micrograph of capsules stabilized by enzyme-nanoparticle conjugates at oil-water interfaces; and e) TEM images of a capsule at low magnification and (inset) high magnification. Reprinted with permission from ref. 29. Copyright 2009 Wiley-VCH.

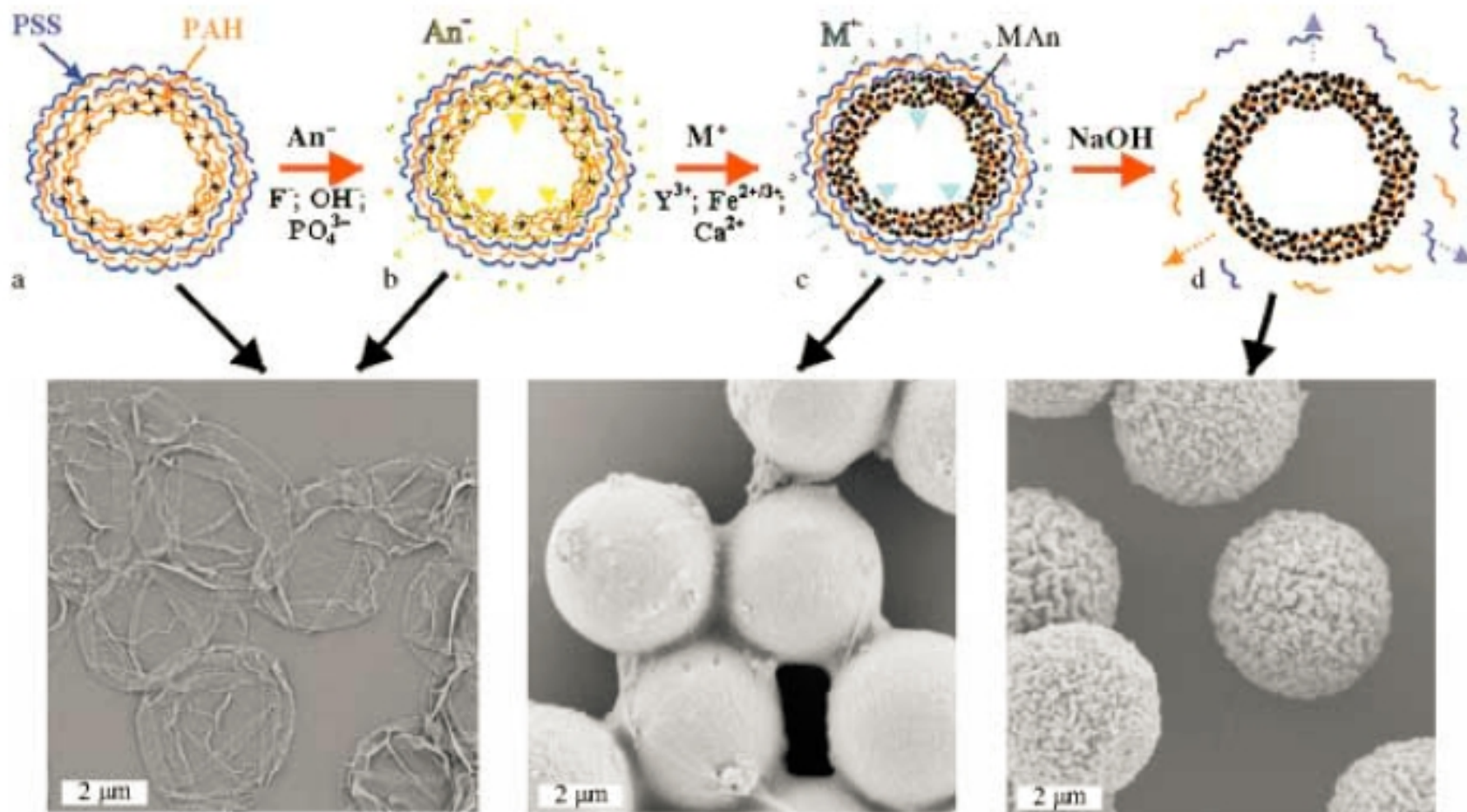


**Fig. S5** Schematic illustration of the preparation of inorganic/organic hollow capsules.  $\text{An} = \text{F}^-$ ,  $\text{OH}^-$ , or  $\text{PO}_4^{3-}$ ;  $\text{M}^+ = \text{Y}^{3+}$ ,  $\text{Fe}^{2+/3+}$ , or  $\text{Ca}^{2+}$ ;  $\text{MAn} = \text{YF}_3$ ,  $\text{Fe}_3\text{O}_4$ , or hydroxyapatite; below: scanning electron microscopy images of the  $\text{YF}_3$  capsules at different preparation stages. Reprinted with permission from ref. 15. Copyright 2003 Wiley-VCH.



## **Description of the synthesize process of the microspheres as shown in Fig. S5**

More specifically,  $\text{MnCO}_3$  microparticles were firstly modified by citric acid, then alternatively assembled with PAH and PSS, and finally treated with EDTA. The resultant PAH/citrate-PAH/PSS capsules were then exposed to a solution containing  $\text{NaOH}$ ,  $\text{H}_3\text{PO}_4$ , or  $\text{HF}$ , thus resulting in the rapid substitution of citrate ions to  $\text{OH}^-$ ,  $\text{PO}_4^{3-}$  or  $\text{F}^-$  ions, and the formation of PAH/ $\text{OH}^-$ -PAH/PSS, PAH/ $\text{PO}_4^{3-}$ -PAH/PSS or PAH/ $\text{F}^-$ -PAH/PSS capsules. Next, the as-acquired capsules were treated with  $\text{FeSO}_4$  and  $\text{Fe}_2(\text{SO}_4)_3$  ( $\text{OH}^-$ -containing capsules),  $\text{CaCl}_2$  ( $\text{PO}_4^{3-}$ -containing capsules), or  $\text{Y}(\text{NO}_3)_3$  ( $\text{F}^-$ -containing capsules) solutions to deposit  $\text{Fe}_3\text{O}_4$ , hydroxyapatite or  $\text{YF}_3$  particles, respectively, inside the capsule wall. The inorganic component in the capsule wall prevented capsule collapse in the dry state, which are reminiscent of those of the original polyelectrolyte capsule in solution.



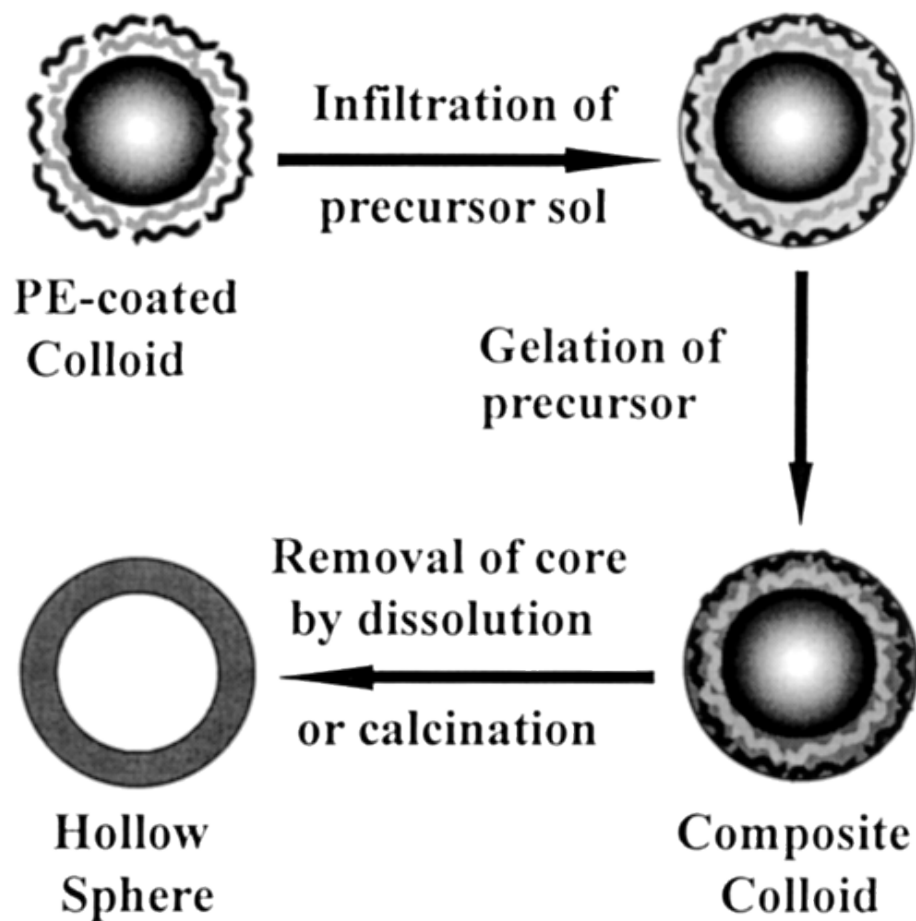


**Fig. S6** Schematic diagram of the procedure used to form the core-shell composite colloids and hollow spheres by using pe-coated colloids as templates. Reprinted with permission from ref. 33. Copyright 2003 Wiley-VCH.

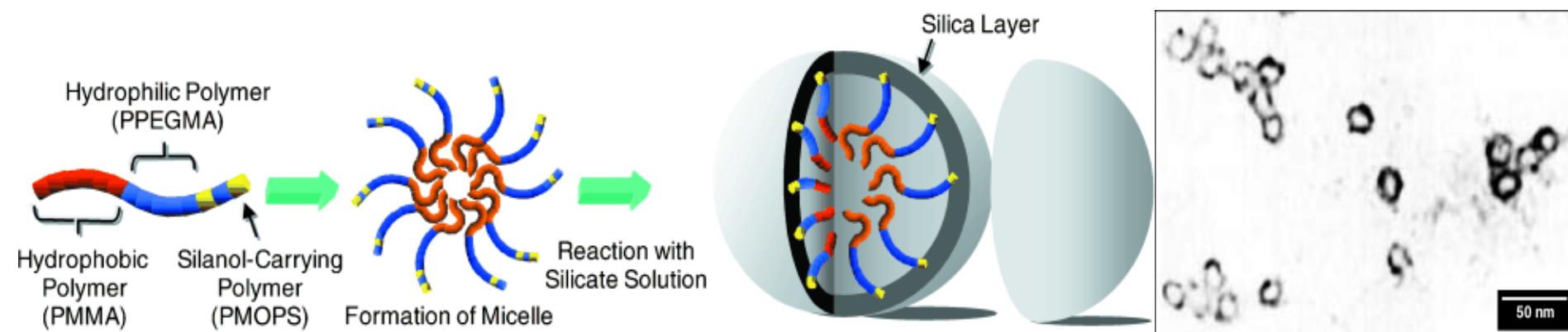


**Fig. S7** Strategy for the synthesis of an organic/inorganic hybrid nanocapsule. Right: TEM image of the organic/inorganic hybrid nanocapsule. Reprinted with permission from ref. 10. Copyright 2003 Wiley-VCH.



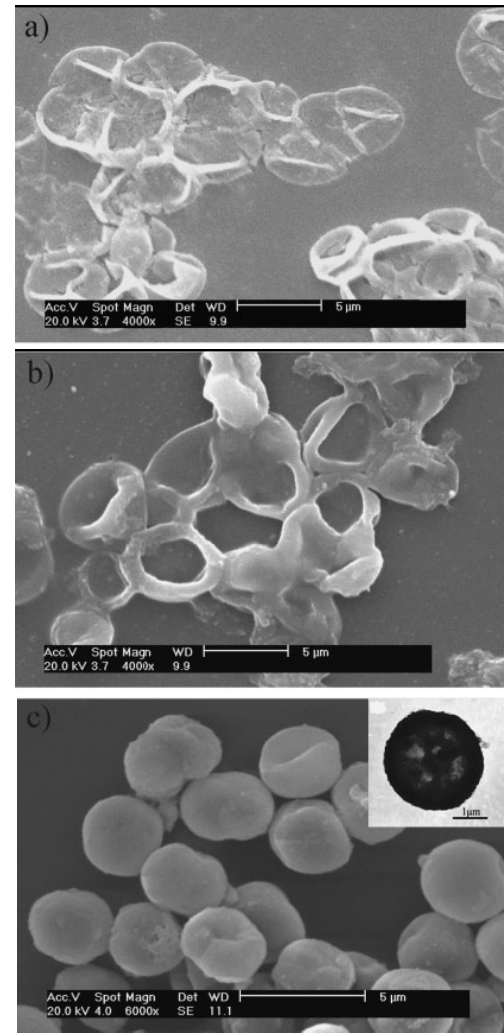
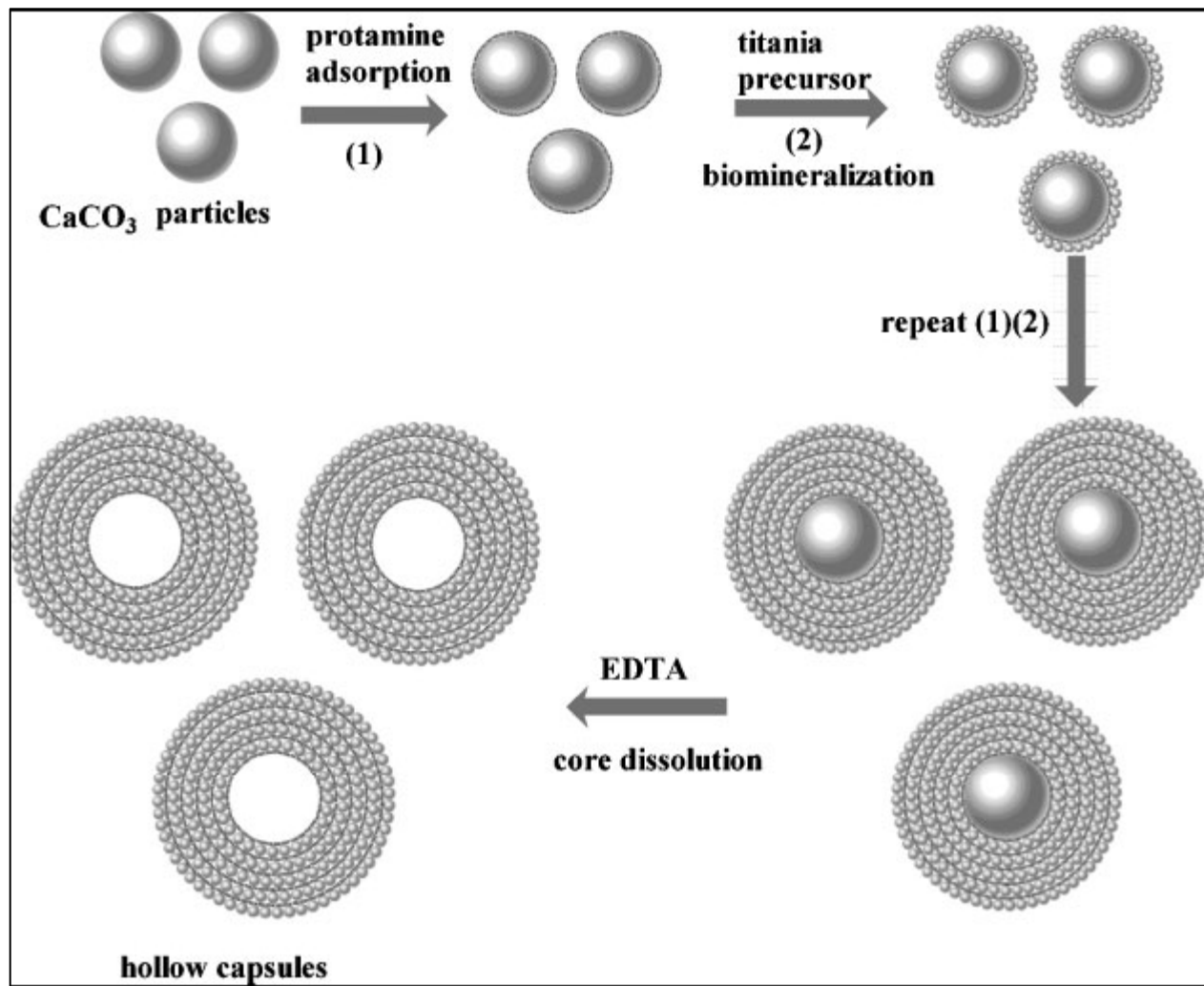


**Fig. S9** Illustration of protamine–titania hybrid microcapsule preparation process. Right: SEM images of hybrid capsules with a) one protamine/titania bilayer, b) three protamine/titania bilayers, and c) five protamine/titania bilayers. Reprinted with permission from ref. 42. Copyright 2009 Wiley-VCH.



**Fig. S10** Schematic illustration of the preparation of PANI-HS@ERGO hybrid capsules. Reprinted with permission from ref. 45. Copyright 2013 American Chemistry Society.

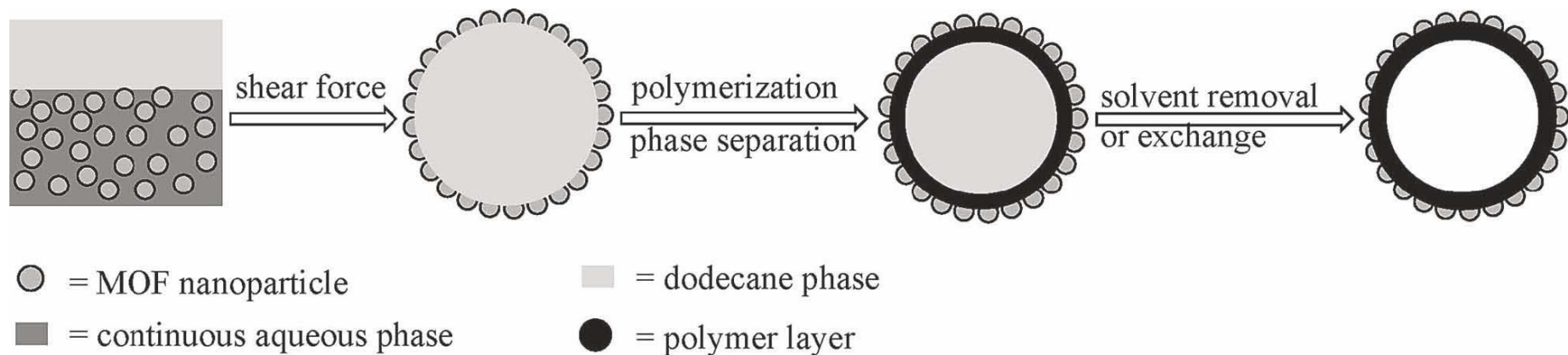


**Fig. S11** Illustration of MOF-polymer hybrid capsule formation. After preparation of a stable "MOFsome" by application of shear force to an aqueous dispersion of MOF nanoparticles and dodecane, the interior is polymerized to form a hollow capsular structure comprised microporous MOF particles embedded within the surface of a polymer shell. Reprinted with permission from ref. 48. Copyright 2013 Wiley-VCH.

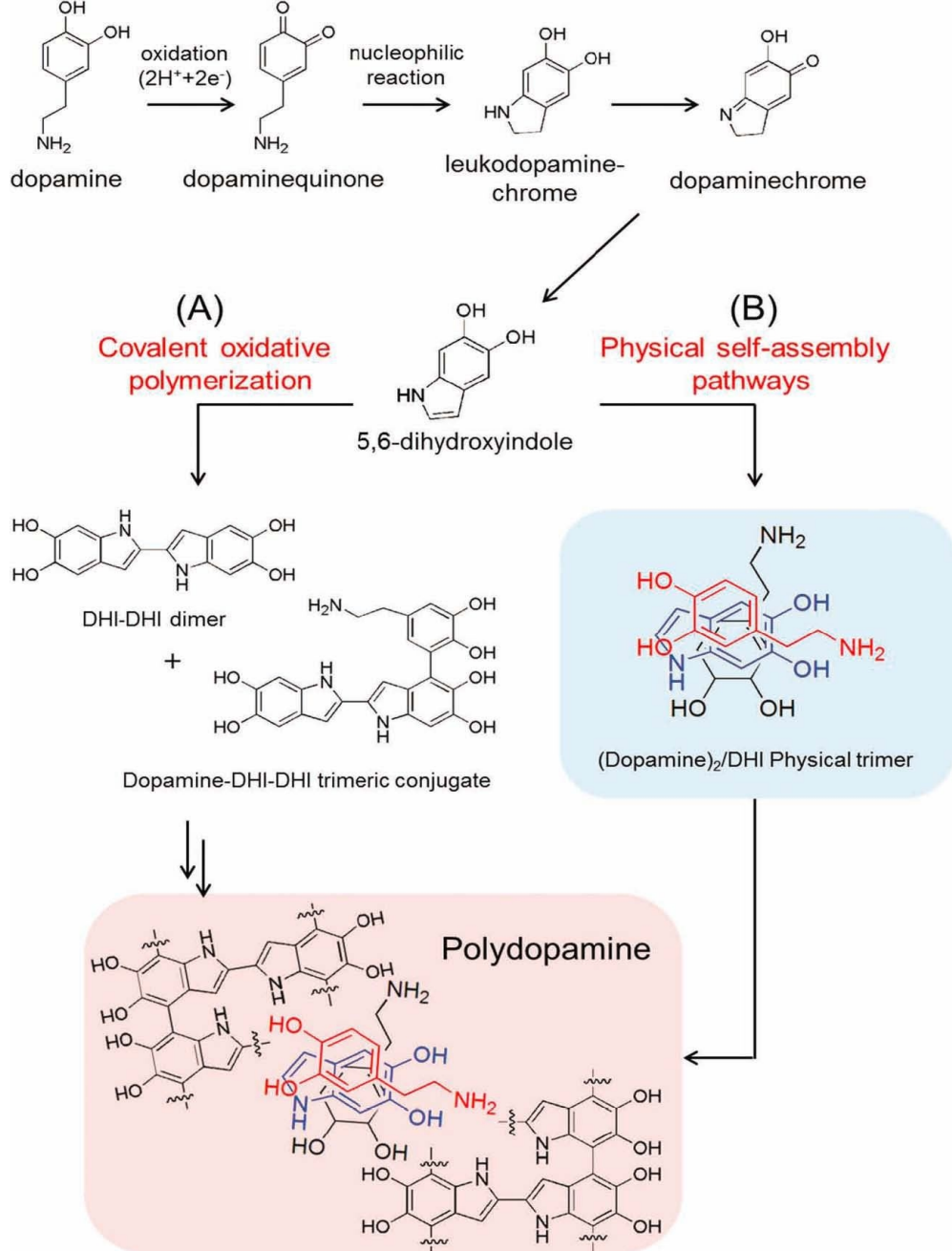


**Fig. S12** Polydopamine synthesis occurs *via* two pathways: A) a pathway of covalent bondforming oxidative polymerization and B) a newly proposed pathway of physical self-assembly of dopamine and DHI. Reprinted with permission from ref. S2. Copyright 2012 Wiley-VCH

**Ref. S2.** S. Hong, Y. S. Na, S. Choi, I. T. Song, W. Y. Kim and H. Lee, *Adv. Funct. Mater.*, 2012, **22**, 4711-4717



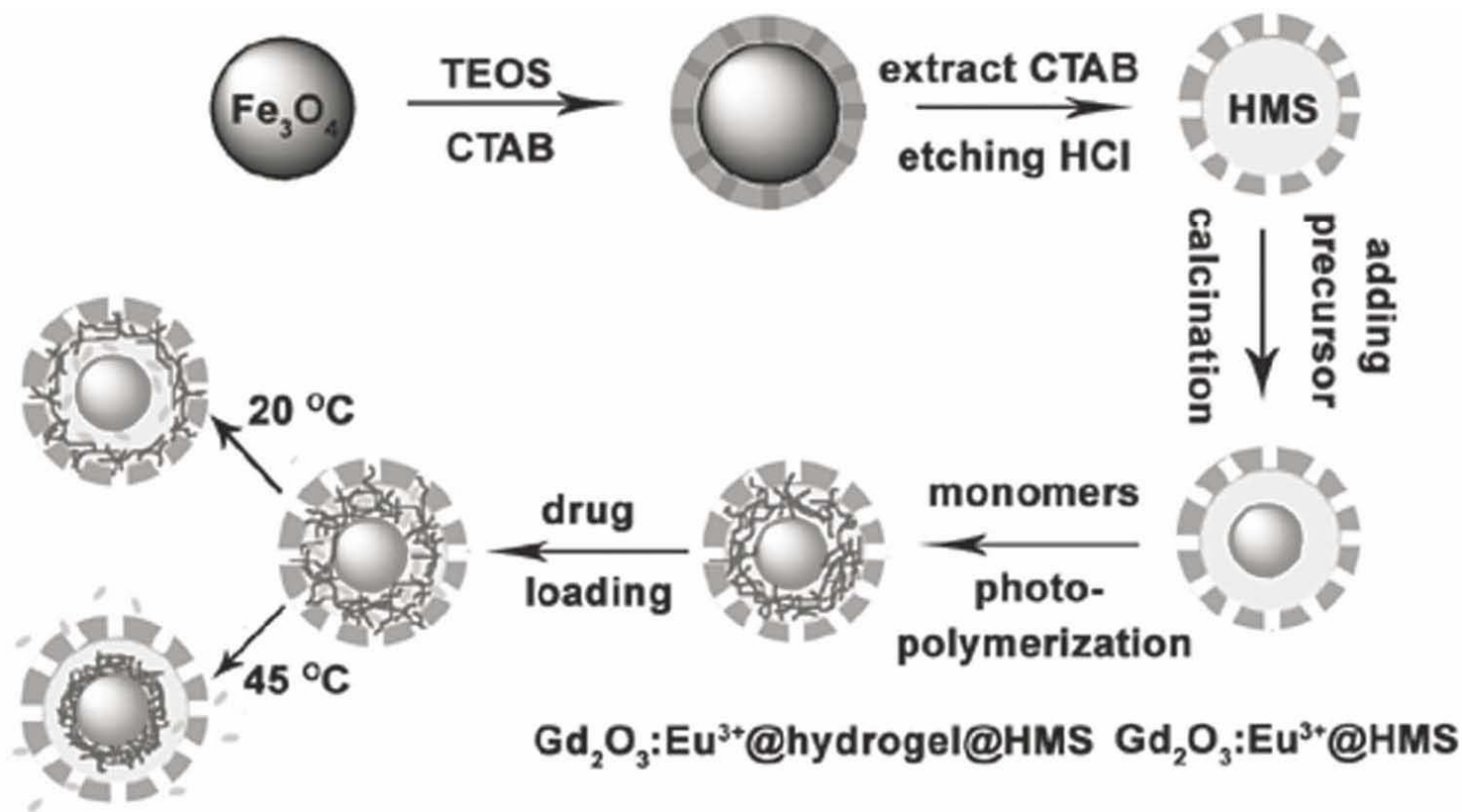


**Fig. S13** Scheme for the synthetic process for P(NIPAm-co-AAm) hydrogel modified luminescent rattle-type mesoporous silica microspheres and subsequent loading and temperature-controlled release of IMC. Reprinted with permission from ref. 50. Copyright 2012 Wiley-VCH.

## **Description of the synthesize process of the microspheres as shown in Fig. S13**

The mesoporous silica capsules were firstly fabricated through conducting the sol-gel reaction of tetraethoxysilane (TEOS) on a sacrificial  $\text{Fe}_3\text{O}_4$  template. Then, gadolinium oxide nanoparticles doped with europium ions ( $\text{Gd}_2\text{O}_3:\text{Eu}^{3+}$ , luminescent nanoparticles) were incorporated into the lumen to form rattle-type mesoporous silica capsules via an incipientwetness impregnation method. Finally, the rattle-type capsules serve as a nanoreactor for filling temperature-responsive hydrogel via photoinduced polymerization to form the multifunctional hybrid microspheres.

## Other references related to the tutorial review

### Assembly of polymers and inorganic particles

1. M. Nakamura, K. Katagiri and K. Koumoto, *J. Colloid Interf. Sci.*, 2010, **341**, 64-68.
2. P. Liu, X. Li, B. Mu, P. Du, X. Zhao and Z. Zhong, *Ind. Eng. Chem. Res.*, 2012, **51**, 13875-13881.
3. F. J. Rossier-Miranda, K. Schroën and R. Boom, *Food Hydrocolloid.*, 2012, **27**, 119-125.
4. A. M. Yashchenok, D. N. Bratashov, D. A. Gorin, M. V. Lomova, A. M. Pavlov, A. V. Sapelkin, B. S. Shim, G. B. Khomutov, N. A. Kotov, G. B. Sukhorukov, *Adv. Funct. Mater.* 2010, **20**, 3136-3142.
5. M. F. Bedard, A. Munoz-Javier, R. Mueller, P. del Pino, A. Fery, W. J. Parak, A. G. Skirtach, G. B. Sukhorukov, *Soft Matter* 2009, **5**, 148-155.

### Assembly of polymers and inorganic precursors

6. R. L. Harbron, T. O. McDonald, S. P. Rannard, P. H. Findlay and J. V. Weaver, *Chem. Commun.*, 2012, **48**, 1592-1594.
7. J. F. Shi, X. M. Zhang, S. H. Zhang, X. L. Wang and Z. Y. Jiang, *ACS Appl. Mater. Interfaces*, 2013, **5**, 10433-10436.

### Assembly of organic precursors and inorganic particles

8. S. Simovic, P. Heard and C. A. Prestidge, *Phys. Chem. Chem. Phys.*, 2010, **12**, 7162-7170.